Phys Chem Minerals (2003) 30: 366–372
DOI 10.1007/s00269-003-0325-3

ORIGINAL PAPER

J. M. Gaite · F. Muller · S. Jemai

Measurements of iron concentration in kaolinites considering disorder broadening of EPR lines

Received: 25 November 2002 / Accepted: 26 April 2003

Abstract Only one part of the EPR lines of a kaolinite spectrum of structural Fe^{3+} is clearly observable because of the overlapping of other lines with other spectra. For this reason, to determine the structural Fe^{3+} concentration we used the line near $g = 9$, although it is not intense. A standard is needed: powders of ZnS containing given concentrations of Mn^{2+} (isoelectronic to Fe^{3+}) were used for this purpose. Using the simulations of the EPR spectra, the concentration (number of Fe^{3+} per Al^{3+}) is determined; it is in the range 10^{-5} to 10^{-4} for our samples. Considering that the crystal-field disorder around Fe^{3+} is responsible for line broadening, we looked for a possible effect of the broadening on the intensity of the EPR spectra. This effect is taken as a distribution of the parameter $\lambda = B_2{}^2/B_2{}^0$. The influence of the parameter λ and its statistical distribution on the position, shape, width and intensity of the EPR line has been calculated using simulation procedures. The correction due to the disorder on the calculated concentration is of the same order of magnitude as the precision measurement. This method can be applied for other kaolinites by comparing the area of their $g = 9$ lines with known ones.

Keywords Kaolinite · EPR · Fe^{3+}

Introduction

Kaolinite is a 1:1 dioctahedric aluminosilicate of formula $Al_2Si_2O_5(OH)_4$. In the octahedral sheet 2/3 of the octahedral sites are occupied by Al^{3+}. Natural samples are more or less disordered, depending on the distribution of Al^{3+} inside the layer, on the abundance of staking faults between the layers and on the presence of impurities or clusters. The physical properties of kaolinite are strongly dependent on its disorder, and several techniques, mainly X-ray diffraction and EPR spectroscopy, were used to study this disorder (Cases et al. 1982). It was supposed that there is a relation between the degree of disorder and the iron concentration in the kaolinites.

The EPR studies of kaolinites showed that the experimental spectrum is the superposition of three different kinds of Fe^{3+} spectra:

- A broad line attributed to a super paramagnetic phase (Bonnin 1982).
- A line at $g = 4.3$ which origin is not surely known (Mestdagh et al. 1982), although the presence of stacking faults and of layers of dickite are partly responsible for this signal (Balan et al. 1999).
- More or less resolved lines arise from Fe^{3+} substituted for Al^{3+}. This iron is called structural iron (Gaite et al. 1993).

It was shown that the line widths of the EPR spectra were strongly dependent on the disorder of the sample and an EPR index based on the observation of the structural iron spectra was proposed to characterize the disorder in the kaolinites (Gaite et al. 1997). This index uses the line width measurements of the $|1/2> \rightarrow |-1/2>$ transition line ($g \cong 9$), which is the only line measurable for most of the kaolinites.

We propose to use this transition line (low field line) to determine quantitatively the structural iron concentration with the help of simulation calculations.

Quantitative EPR is a complex problem, for the signals depend on several experimental parameters such as the position of the sample inside the cavity, the Q factor of the cavity etc., as described by Nagy (1993) and Yordanov (1994).

J. M. Gaite · F. Muller (✉)
Institut des Sciences de la Terre d'Orléans,
Université d'orléans – CNRS,
1A rue de la Férollerie F-45071 Orléans Cedex 2
Tel. : +33-238-255-397
Fax: +33-238-636-488
e-mail: Fabrice.Muller@univ-orleans.fr

S. Jemai
Laboratoire de Physique des Matériaux,
Faculté des Sciences de Bizerte,
7021 Zarzouna Tunisie

Another difficulty of quantitative EPR is the choice of a standard. Several carbon-based standards were proposed by Auteri et al. (1994). In a previous study of Fe^{3+} in kaolinite Balan et al. (2000) used standards of Fe^{3+}-doped αAl_2O_3. We looked for the possibility to use Mn^{2+} which is iso-electronic to Fe^{3+}. Mn^{2+} in several MO compounds is listed by Yordanov (1994). In this work we used ZnS samples containing various concentrations of Mn^{2+} as standards.

The intensity of the EPR spectra is proportional to the concentration; however, nothing is known about a possible influence of the crystal-field disorder. This aspect will be developed in this paper.

Experiments

EPR spectroscopies

The EPR spectra were recorded with a double-cavity Varian 4502 and using a 100-kHz modulation. The magnetic field was calibrated using an NMR Gaussmeter, and the frequency was precisely measured using an HP frequency meter. In order to obtain quantitative measurements of the intensities, we controlled the modulation and the receiver gain calibrations, and all experimental parameters were carefully controlled. The EPR spectra were digitized and recorded in a computer. All experiments were performed at room temperature. To circumvent sample position dependency on the EPR signal, samples were placed inside calibrated cylindrical silica tubes inside the cavity. They occupy all the cavity height and their mass density was measured. To avoid any variations of signal intensity with the position of the tube inside the cavity, we used specific tube holders. We controlled that there was no preferential orientation of the kaolinite particles inside the tube. The same procedure was used for the kaolinite samples and for the standards.

The samples

The kaolinites used in this work were previously studied by Gaite et al. 1997 (DCV and GB3 samples) and by Razafimandiby et al. 1982 (IBITY sample from Madagascar). The spectra of these samples characterized by different disorder parameters are presented in Fig. 1.

The standards

The simplest way to determine the Fe^{3+} concentration in a given powdered sample is to compare the intensity of the spectrum (or the same lines of the sample) with that of a standard containing a known amount of Fe^{3+} submitted to a similar crystal field, i.e. having a similar spectrum. For kaolinite, such standards could be Fe^{3+} in ZrO_2 or in $YAlO_3$; unfortunately, in spite of great efforts, such samples were not available, and we used a more complicated method. As standards we used powders of ZnS doped with Mn^{2+} with various concentrations. We had eight different specimens with an [Mn/Zn] ratio varying between 2.5×10^{-5} and 2.5×10^{-3}. The spectra of two of these standards ([Mn/Zn] = 7.5×10^{-5} and 7.5×10^{-4}) are presented in Fig. 2a.

Basis of the method

Our purpose is to use both experimental and simulated spectra. The aim is to use a ratio (R_M) of some characteristics of the experimental spectra of the samples and of a standard. R_M is then compared to the same ratio (R_T) calculated from simulated spectra.

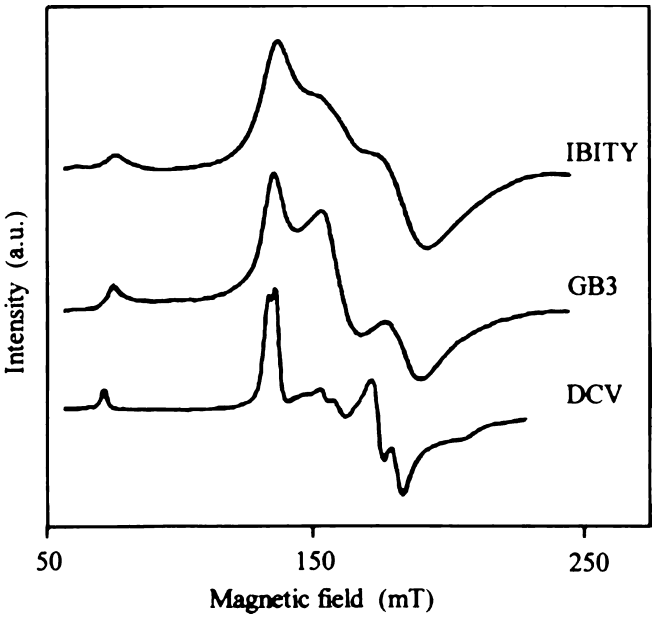

Fig. 1 X-band frequency experimental spectra of the three samples

The different steps of this method are detailed below. The main characteristic of the Fe^{3+} spectra (Fig. 1) is the presence of the low field line isolated from the others. The area I_K of this line is proportional to the Fe^{3+} concentration in the sample. It was used to characterize the sample disorder and to carry this present study. Of course, one line belonging to the Fe I spectrum exists near $g = 9$, as Fe I is characteristic of an important crystal-field disorder; this line is very broad and is included in the base line. It is observed in the spectra of the standards (Fig. 2a) that the intensities depend on the Mn^{2+} concentration but also on the lines widths because of the dipolar broadening. The only characteristic of the Mn^{2+} spectra is related to the whole spectrum, having an intensity I_Z. The Mn^{2+} concentration of the standards was checked by double integration of the recorded spectra. The first integration of the spectrum (the absorption curve) for two different standards is presented in Fig. 2b. The second integration gives the signal intensity. To check our standard, we calculated the intensities for several standards. The plot of the intensity of the Mn^{2+} spectra as a function of the (Mn/Zn) ratio is presented in Fig. 3. This curve shows a good linear relation between the intensity and the concentration, indicating that the standards are well calibrated. For further measurements we used the standards with concentration [Mn/Zn] = 7.5×10^{-4}. We determined the ratio $R_V = I_K/I_Z$. This ratio is related to the same sample volume; it can be transformed into the same mass ratio R_M, by the relation:

$$R_M = R_V \times \frac{D_K}{D_Z} \ ,$$

where D_K and D_Z are, respectively, the mass densities of the sample and of the standard inside the silica tube. The measured areas are proportional to the concentration of paramagnetic species and R_M is also given by:

$$R_M = k \times [Fe^{3+}]/[Mn^{2+}] = k \times C_K/C_Z = k \times N_K/N_Z \ ,$$

where k is a constant. C_K and C_Z are, respectively, the concentrations of Fe^{3+} in the sample and of Mn^{2+} in the standard. N_K and N_Z are, respectively, the spin numbers per unit mass in the sample and in the standard. The constant k was determined with the simulated spectra of the samples and the standard with [Mn/Zn] = 7.5×10^{-4}.

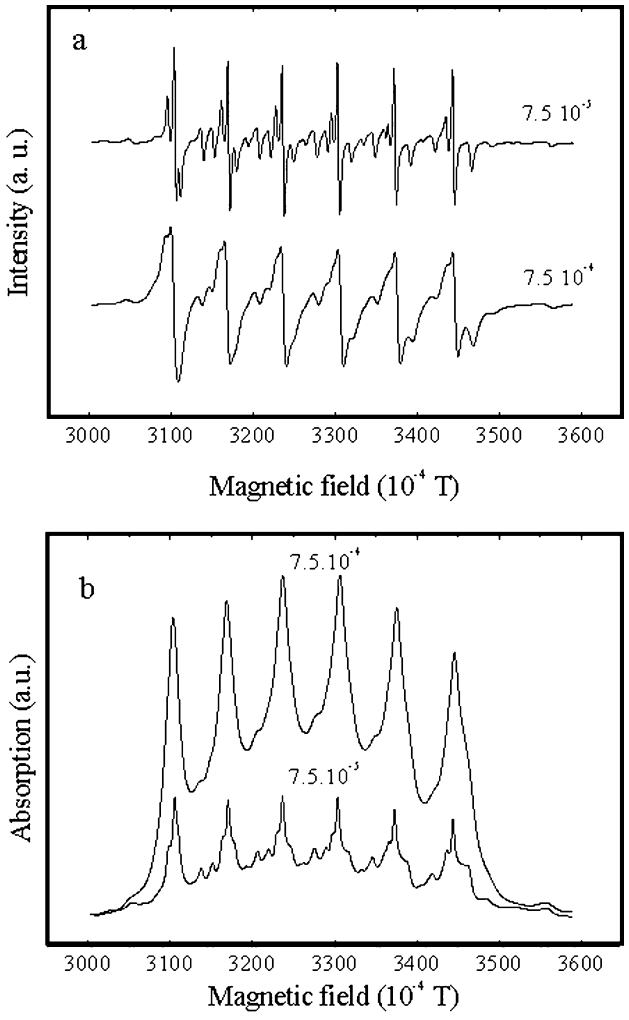

Fig. 2 X-band frequency experimental spectra of two standards with $[Mn]/[Zn] = 7.5 \times 10^{-5}$ and 7.5×10^{-4} (**a**) and their numerical integration (**b**)

Simulations of the EPR spectra

The sample spectra

The EPR spectra of powdered kaolinites were simulated using a home-made procedure with two main steps.

The simplified spin Hamiltonian of Fe^{3+} in kaolinite is given by: $H = \sum_i g\beta B_i S_i + B_2^0 O_2^0 + B_2^2 O_2^2$ (Abragam and Pryce 1951),

where O_2^m ($m = 0, 2$) are the Stevens equivalent operators (Abragam and Bleaney 1970), B_2^m are the fine structure constants, B_i are the components of the magnetic field, S_i the spin operators and β is the Bohr magneton. We computed the absorption spectra, using the constants B_2^0 and B_2^2 of the structural iron in kaolinite determined previously (Gaite et al. 1993; Balan et al. 1999) and an isotopic g value ($g = 2$) considering no line shape or width, i.e. considering the line shape as a δ function (Fig. 4a).

In a second step we convoluted the absorption curve by the derivative of a normalized line shape (either Gaussian or Lorentzian); a simulated EPR spectrum is then obtained (Fig. 4b). In this way, the area of the $g = 9$ line is independent of the shape and width; it is obtained in arbitrary units depending mainly on the number of orientations used for the simulation of the spectra. The area I_{KT} of the low field line of the simulated spectra is then calculated by integration.

This procedure has been described previously for Fe^{3+} (Gaite et al. 1993) and for Cr^{3+} (Gaite and Mosser 1993).

The standard spectrum

We used the same program to calculate the intensity of the Mn^{2+} spectrum in ZnS with some assumptions:

We treated Mn^{2+} like its iso-electronic Fe^{3+}, that means we simulated the absorption curve of Mn^{2+} (like Fe^{3+}) neglecting the hyperfine splitting arising from the 5/2 nuclear spin of ^{55}Mn, and using the spin Hamiltonian parameters of Mn^{2+} in ZnS given by Low (1960). As in sample simulation, we used an isotopic g value ($g = 2$) considering no line shape and the same number of orientations, i.e. the same number of spins.

For this case, we did not use the second step of the procedure for kaolinite as we did not have to simulate the spectra. To obtain the intensity I_{ZT} of the spectra we directly integrated the absorption curve.

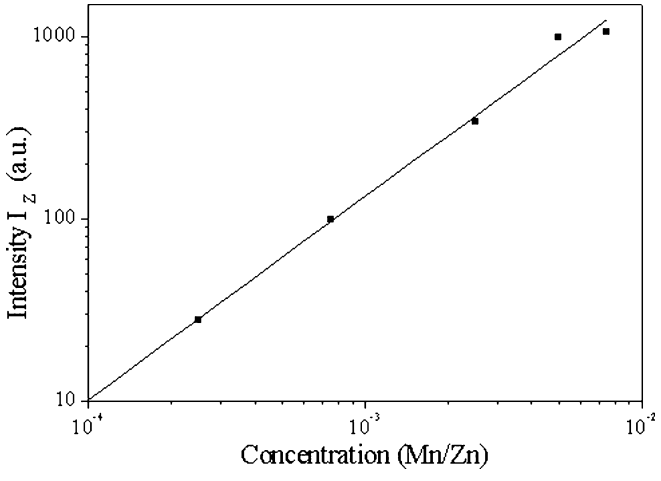

Fig. 3 Intensity I_Z of the standard spectra as a function of the [Mn]/[Zn] ratio

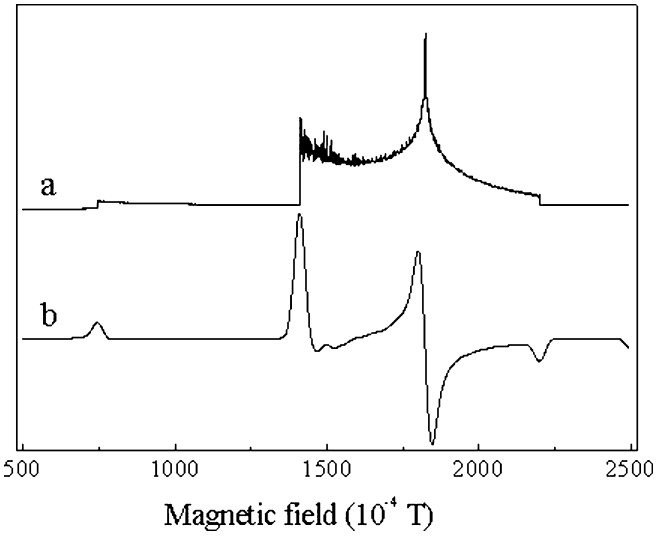

Fig. 4 Simulated absorption spectra of a kaolinite sample (**a**) and its derived curve (**b**)

The ratio of the area of the $g = 9$ line I_{KT} in simulated kaolinite to the intensity one I_{ZT} of the theoretical standard is given by: $(I_{KT}/I_{ZT}) = R_T$.

For simulations done with the same number of spins for the samples and the standard, we have $R_T = k$ then:

$$N_K = N_Z \cdot \frac{R_M}{R_T} \ .$$

The concentration of structural Fe^{3+} in kaolinite is then given by:

$$[Fe^{3+}]/[Al^{3+}] = ([Mn^{2+}]/[Zn^{2+}]) \times (M_K \cdot R_M)/(4 \cdot M_Z \cdot R_T) \ ,$$

where M_k is the mass of the structural formula of kaolinite and M_Z is that of ZnS. The 4 factor in the preceding expression arises from the presence of 4 Al^{3+} in the structural cell of the kaolinite.

Results

The results are presented in Table 1. For the GB3 sample we did two experiments under different conditions (GB3-1 and GB3-2) to test the precision and reproducibility of the method. The concentrations measured for these specimens are within a 10% range (see Table 1). We may then assume that the precision of the measurement is of the order of 10%. Our results are much lower than those obtained by Balan et al. (2000) (20 times for the DCV sample). In fact, Balan et al. (2000) determined the concentration of Fe^{3+} giving both Fe I and Fe II spectra. However, the difference seems too great to be explained only by the amount of iron giving the Fe I spectrum, and there must be other reasons not yet explained.

In such a calculation, it was assumed that the intensity of the $g = 9$ transition in kaolinite is independent of its line width, i.e. of the crystal-field disorder of the sample. We then looked for a possible influence of crystal-field disorder on the intensity of the EPR spectra.

Influence of crystal-field disorder

Looking for a possible influence of the crystal-field disorder on the intensities of the EPR lines, in a first step, we considered that this effect is mainly responsible for the line width, i.e. we did not consider any dipolar broadening.

Any change in the environment of Fe^{3+} will produce a variation of the fine structure spin Hamiltonian constants; mainly it can be a change of the second-order constants that can be expressed as a change of the constants B_2^0 and B_2^2 and the eigenvector orientations of the second-rang tensor (Gaite et al. 1993). This last effect has not to be taken into account, because we are concerned with powders. The zero field splitting being much greater than the hyperfrequency energy, the magnetic field positions are mainly sensitive to the ratio $\lambda = B_2^0/B_2^2$ (Gaite et al. 1993). A crystal-field disorder can then be considered as a distribution function of the parameter λ. As the disorder can be considered as statistical, we described it by a normalized Gaussian distribution of the λ parameter, $G(\lambda)$.

To test the influence of λ on the spectra, we first computed the absorption curve of Fe^{3+} for different and equally spaced values around $\lambda_0 = 0.67$, which is the calculated value for very well-ordered kaolinites. The low field part of the simulations is presented in Fig. 5, which is the basis of our calculations. The curves are noisy because no line shape was used, i.e. each transition is considered as a Dirac, the noise depending on the number of orientations used to simulate a powder and on the choice of the spectra resolution.

Looking at one of these curves (Fig. 5), if the small discontinuity at low field (at a lower field than the one studied) corresponding to the transition $|5/2> \rightarrow |-5/2>$ for $B \ // \ O_Z$ is neglected, it may be schematized as presented in Fig. 6. The absorption curve may be described by:

$$A(B, \lambda) = I_m(\lambda) f(B, \lambda) \Upsilon(B - B_m) \ ,$$

where I_m is the absorption at the B_m discontinuity, $\Upsilon(B-B_m)$ is the Heaviside function and $f(B, \lambda)$ is the shape of the curve to the right of the discontinuity.

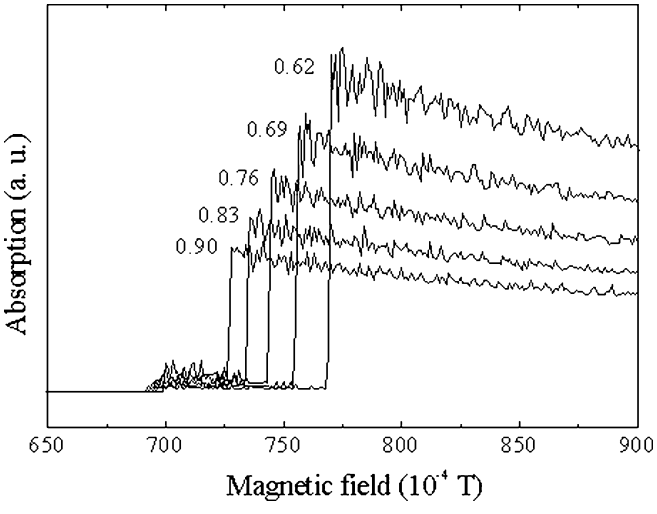

Fig. 5 Simulated absorption spectra of a kaolinite sample for different λ values

Table 1 Main characteristics of the low field part of the EPR spectra for different samples and calculated concentration expressed in number of iron per aluminium

Sample	Intensity (a.u.)	Width at half maximum (mT)	Concentration $[Fe^{3+}]/[Al^{3+}]$
DCV	83×10^{-8}	2.1	49.2×10^{-6}
GB3–1	126×10^{-8}	5.3	74.7×10^{-6}
GB3–2	130×10^{-8}	5.3	77.0×10^{-6}
IBITY	620×10^{-8}	6.4	330.0×10^{-6}

The EPR signal being the derivative of the absorption curve, the simulated EPR signal is given by:

$$S(B,\lambda) = I_m(\lambda)\delta(B - B_m) + I_m(\lambda)\Upsilon(B - B_m)\frac{\partial}{\partial B}f(B,\lambda) \ .$$

The simulated EPR spectrum will depend on the parameters I_m, B_m, and on the shape of the function $f(B, \lambda)$. We have then to determine the variations of these parameters with λ.

From Fig. 7, it is observed that there is a linear relation between I_m and B_m. Inside the observation range of the $|1/2> \rightarrow |-1/2>$ transition, the right side of the absorption curve may, in a first approach, be assimilated to a straight line with a slope $\alpha(\lambda)$ [or $\alpha(B_m)$], λ and B_m being dependent (Fig. 6). With these considerations the signal $S(B, \lambda)$ becomes:

$$\begin{aligned} S(B,\lambda) &= I_m(\lambda)\delta(B - B_m) + \alpha(\lambda)\Upsilon(B - B_m) \\ &= S_1(B,\lambda) + S_2(B,\lambda) \ . \end{aligned}$$

Figure 8 shows a linear variation of $\alpha(\lambda)$ with the magnetic field B_m. There is no simple evident relation between the parameters λ and B_m, so the relation between them must be fitted by a polynomial (or nearly so) expression. The best fit we obtained, avoiding high polynomial orders, is indicated in Fig. 9.

For any distribution $G(\lambda)$ of the crystal field, the simulated EPR spectrum is given by:

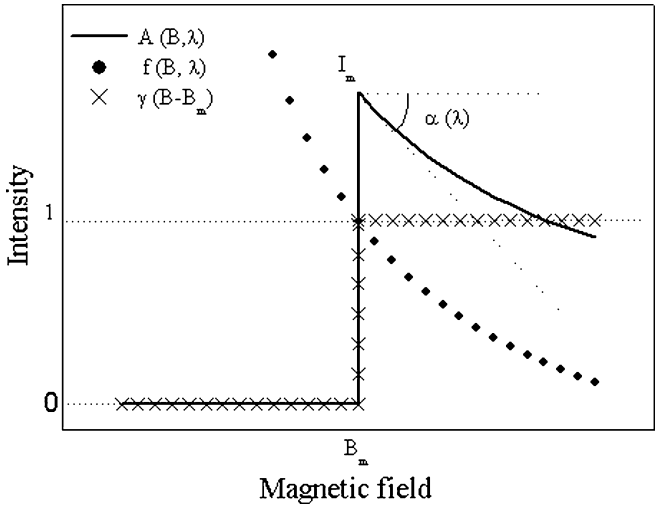

Fig. 6 Schematic representation of the method used to simulate the absorption curve of kaolinite samples

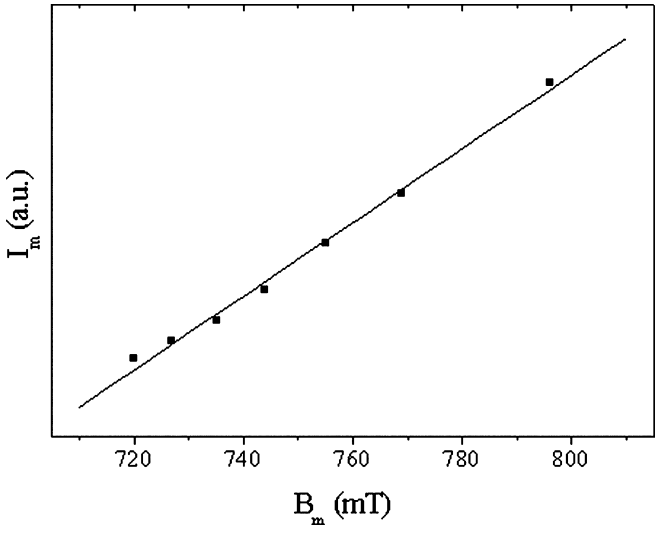

Fig. 7 A representation of the I_m intensity as a function of the discontinuity position B_m. A linear relation between I_m and B_m is $I_m = -83 + 0.1197\ B_m$. B_m is expressed in 10^{-4} T (frequency: 9615 MHz)

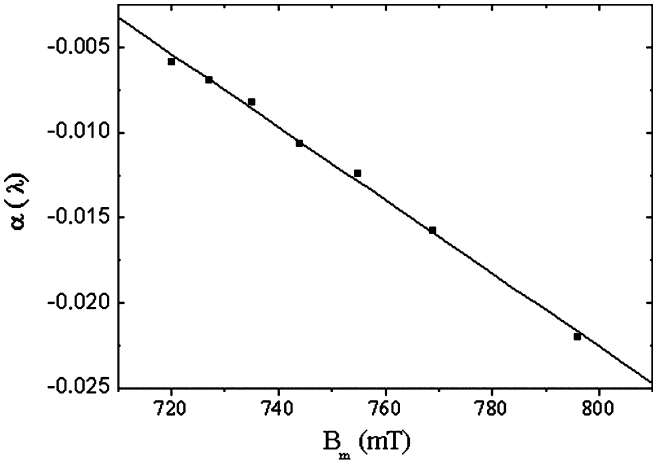

Fig. 8 A representation of the slope $\alpha(\lambda)$ as a function of the discontinuity position B_m. A linear relation between $\alpha(\lambda)$ and B_m is $\alpha(\lambda) = 0.149–0.00021\ B_m$

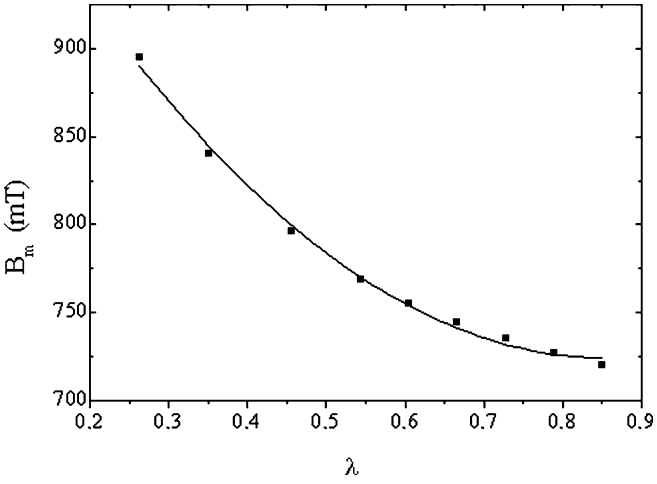

Fig. 9 The magnetic field B_m as a function of the λ values. A polynomial relation between B_m and λ is $B_m = 1071.02 - 811.58\ \lambda + 474.56\ \lambda^2$

$$Y(B) = \int_0^1 S(B,\lambda)G(\lambda)\mathrm{d}\lambda$$
$$= \int_0^1 S_1(B,\lambda)G(\lambda)\mathrm{d}\lambda + \int_0^1 S_2(B,\lambda)G(\lambda)\mathrm{d}\lambda$$
$$= Y_1(B) + Y_2(B) \ .$$

To obtain the simulated EPR spectra, we used a Gaussian distribution:

$$G(\lambda) = (a/\sqrt{\pi})\exp[-a^2(\lambda - \lambda_0)^2] \ ,$$

where a is the dispersion parameter and λ_0 is the rhombicity parameter for a kaolinite (0.76).

For convenience, we studied separately the two parts $Y_1(B)$ and $Y_2(B)$ of $Y(B)$. $Y_1(B)$ makes a contribution to the signal with a zero base line, while $Y_2(B)$ mainly influences the base line. These effects are well illustrated by the example shown in Fig. 10. The integral of $Y_1(B)$ is easy to calculate and does not differ much from that of $Y(B)$. Then for calculations we used $Y_1(B)$, which fits the spectrum well.

The shapes of the simulated signals $[Y_1(B)]$ are presented in Fig. 11 for various values of the dispersion parameter a. In this figure, it is observed that when the line width increases, the line becomes more and more dissymmetric and that there is a slight shift of the maximum of the line. The integration of the $Y_1(B)$ signal for the different values of the a parameter let us plot the area of the $g = 9$ calculated line versus the line width (Fig. 12).

Discussion

For a given signal, the line width depends on the crystallinity of the sample (Gaite et al. 1993). Because the DCV kaolinite is considered as a well-crystallized sample, it is assumed that its line width (L_{DCV}) is the minimum that we can obtain, the width being due to relaxation and also to the fact that this line is the sum of two neighbouring lines arising from Fe^{3+} at the two Al positions (Gaite et al. 1993). Then the measured line width of a given sample (L) includes the contribution of L_{DCV} and a widening due to the disorder (L_{disorder}) as calculated previously (Fig. 12). So we measured for each sample the line width L and determined the L_{disorder} with the relationship $L_{\mathrm{disorder}} = L - L_{\mathrm{DCV}}$. These obtained values are reported on the curve in Fig. 12 to evaluate the correction coefficient. The corrections are 5 and 8%, respectively, for the GB3 and IBITY samples. For example, for IBITY sample the concentration is $[Fe^{3+}/Mn^{2+}] = 3.30 \times 10^{-4}/1.08 = 3.06 \times 10^{-4}$. This correction is of the order of the precision of the measurement and it can be concluded that the disorder does not effectively change the area of the $g = 9$ line.

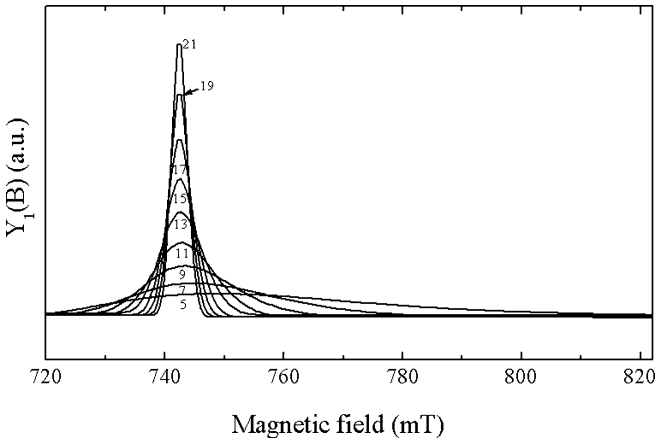

Fig. 11 Simulated signals shapes $[Y_1(B)]$ for various values of the a parameter of the Gaussian distribution. The a values are given *below the corresponding curve*

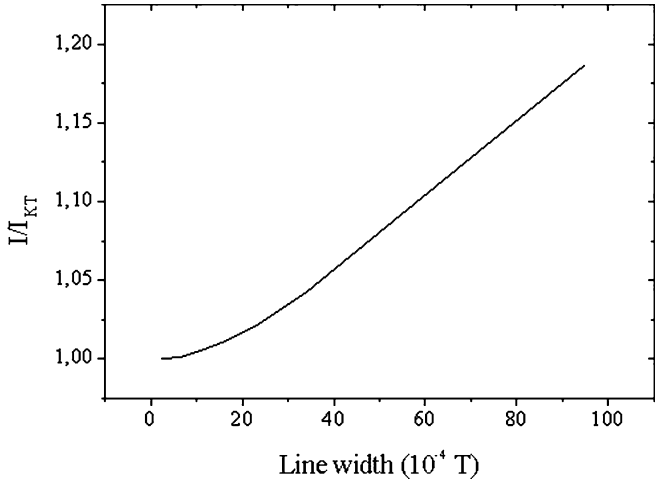

Fig. 12 A representation of the calculated relative area I/I_{KT} of the $g \cong 9$ line as a function of the line width. I is the area of the calculated $g \cong 9$ line and I_{KT} is that for a Dirac line shape

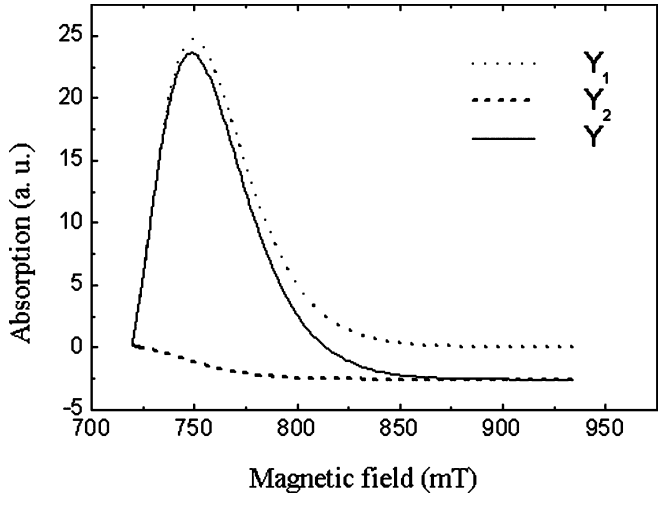

Fig. 10 A representation of $Y_1(B)$, $Y_2(B)$ and $Y(B) = Y_1(B) + Y_2(B)$ functions used for the EPR simulation with $\nu = 9615$ MHz and $a = 7$

Conclusion

The method we presented allows the measurement of the concentration of the structural Fe^{3+} (at Al position) in kaolinites. The line width of the spectrum depending on the disorder of the sample, it is observed that for the same concentration the area of the low field line increases slightly with the disorder.

Even for wide lines (less than about 10 mT) the increase of the area due to the disorder does not change the order of magnitude of the concentration calculated in the first step. For the very disordered samples, the EPR lines are much broadened; the $g \cong 9$ line is no longer isolated and it is not possible to use it for the calculation.

In the present paper we did not measure a large amount of samples, but for other samples it is not necessary to repeat such experiments, as it is sufficient to compare directly the area of the line of the new sample with that of a known one (DCV, GB3, IBITY).

References

Abragam A, Pryce MHL (1951) Proc Roy Soc, GB (A) 205: 135

Abragam A, Bleaney B (1970) Electron paramagnetic resonance of transition ion. Clarendon, Oxford, pp 133–149

Auteri FP, Beldford RL, Boyer S, Motsegood K, Smirnov A, Smirnova T, Vahidi N, Clarkson RB (1994) Carbon-based standards for electron paramagnetic resonance spectroscopy. Appl Magn Reson 6: 287–308

Balan E, Allard Th, Boizot B, Morin G, Muller JP (1999) Structural Fe^{3+} in natural kaolinite: new insights from electron paramagnetic resonance spectra fitting at X- and Q-band frequencies. Clays Clay Miner 47: 605–616

Balan E, Allard Th, Boizot B, Morin G, Muller JP (2000) Quantitative measurement of paramagnetic Fe^{3+} in kaolinite. Clays Clay Miner 48: 439–445

Bonmin D, Muller S, Calas G (1982) Le fer dans les kaolinites: Etude par spectroscopie RPE, Mössbauer, EXAFS. Bull Mineral 105: 467–475

Cases JM, Liétard O, Yvon J, Delon JF (1982) Etude des propriétés cristallochimiques, morphologiques, superficielles de kaolinites désordonnées. Bull Mineral 105: 439–455

Gaite JM, Mosser C (1993) Experimental and modelized electron paramagnetic spectra of Cr^{3+} in kaolinite. J Phys (C) 5: 4929–4934

Gaite JM, Ermakoff P, Muller JP (1993) Characterization and origin of two Fe^{3+} EPR spectra in kaolinite. Phys Chem Miner 20: 242–247

Gaite JM, Ermakoff P, Allard Th, Muller JP (1997) Paramagnetic Fe^{3+}: a sensitive probe for disorder in kaolinite. Clays Clay Miner 45: 496–505

Low W (1960) Paramagnetic resonance in solids. Academic Press, New York, pp 118–118

Mestdagh MM, Herbillon AJ, Rodrique L, Rouxhet PJ (1982) Evaluation du rôle du fer structural sur la cristallinité des kaolinites. Bull Mineral 105: 457–466

Nagy V (1994) Quantitative EPR: some of the most difficult problems. Appl Magn Reson 6: 259–285

Razafimandiby A, Rakotomaria E, Rautureau M, Caillère S (1982) Etude de la kaolinite du mont Ibity (Madagascar). 107ème Congrès national des sociétés savantes, Brest, Sciences, Fasc III: 387–398

Yordanov ND (1994) Quantitative EPR spectrometry – state of the art. Appl Magn Reson 6: 241–257